VENTED GAS EXPLOSIONS IN A LONG VESSEL WITH OBSTACLES

A. Alexiou, H. Phylaktou, and G. E. Andrews
University of Leeds, Department of Fuel and Energy, Leeds LS2 9JT

Methane / air explosions in long open-end vessel were undertaken in order to investigate the effects of obstacles (20% - 80% blockage ratio) in vented explosions and also to compare with previous findings in totally confined vessels. Three pressure peaks were identified: Pressure peak P_1 was due to a fast elongated flame prior to the flame reaching the obstacle; pressure peak P_2 due to the turbulence created by the obstacle; Pressure peak P_3 due to the external explosion. All the pressure peaks increased with increasing blockage up to about 60%. Different behaviour was recorded with 80% blockage and some possible explanation for this is provided. The rates of pressure rise due to the obstacle showed similar trends i.e. increased with increasing blockage ratio up to 60%. The normalised rates (relative to the no - obstacle rate) were found to be in good agreement with those measured previously in the totally confined tests. This demonstrates the validity of assessing the effect of obstacles in totally enclosed tests. Unburned gas velocities were measured and the turbulent factors were evaluated on the basis of fundamental turbulent combustion parameters and were found to be in good agreement with the enhancement factors obtained from the normalised rates of pressure rise. The present reported turbulent factors were at least two times higher than the current turbulent factors suggested in literature for compact vessels and consequently a need for revising the current venting guidelines is recommended for large L/D vessels with obstacles.

Key words: Gas explosions, venting, obstacles

INTRODUCTION

Pressure relief vents are widely used in the process industries to protect the vessels from accidental explosion damage. Adequate venting area must be provided to ensure that the pressure is released sufficiently fast to counter the rate of pressure generation by the combustion process. The maximum rate of pressure rise, during an accidental explosion, is therefore a vital parameter in determined the correct size of the vent area. The rate of pressure rise is a function of the vessel shape and volume, the mixture composition and any turbulence-promoting obstacles in the path of the flame. In current pressure relief vent design practice, for compact vessels, the effect of obstacles induced turbulence is allowed for, by the introduction of a turbulence factor, β. This is done by using a value of turbulent burning velocity, S_T, in the empirical equations, which is related to the laminar burning velocity, S_L, by:

$$S_L = \beta S_T \qquad (1)$$

Although some values for β were suggested by Rasbash et al (1), experimentally determined values are sparse and none exist for large length to diameter ratio (L/D) vessels. This is

recognised in explosion venting guidelines such as NFPA 68 (2) which is totally based on the suggested values of Rasbash et al (1), ranging from 1.5 to 5 depending upon the type of enclosure and the type of obstacles. In the case of severe turbulence they suggested values of the turbulence factor ranging from 8 to 10. Phylaktou and Andrews (3) quantitatively determined the influence of obstacles on flame propagation in large L/D completely closed vessel explosions. They reported values of the turbulent factor as high as 110, induced by a single orifice plate which was over ten times higher than the maximum value currently recommended for severe cases of turbulence by Rasbash et al (1) for explosions in near cubical volumes.

In the present paper the effect of an obstacle in a vented large L/D vessel explosion was evaluated. Turbulence factors were measured and calculated from the estimates of the turbulent burning velocities and compared with those measured in a totally enclosed vessel.

EXPERIMENTAL

The tests were carried out in a cylindrical vessel of 0.076 m of diameter constructed from 0.5 m long flanged sections. The length to diameter ratio (L/D) was constant at 20.4. The vent was a fully open end, $K_V = 1$, (K_V is the vent coefficient which is equal to $K_V = A_T / A_V$ where A_T is the flow - cross sectional - area of the tube and A_V is the area of the vent). The ignition was at the centre of the opposite end of the vessel to the vent. The vent was mounted in the end flange opposite to the ignition. The explosion was vented into a dump vessel 0.5 m diameter 1.0 m long vessel filled with air at 1 bar, which was connected with a pipe of 0.162 mm of diameter 1.5 m long to another air filled vessel of 0.5 m diameter 2 m long as is shown in Figure 1. This was used as a dump volume to allow safe venting experiments in the laboratory. This configuration gave a test to total volume ratio of about 90 which is much larger than the required (estimated about 10) to give a realistic simulation of tests vented to open atmosphere. An aluminium gate vacuum valve was used to separate the test section from the dump sections. The gas/air mixture was formed by partial pressures and a homogenous composition was achieved by circulating the mixture in the explosion vessel using an external recirculating pump. The initial pressure in both sections (test section and dump section) was 1 atm and the gate valve was opened just prior to the ignition of the explosion, thus any movement of gases or air from one section to another was restricted. The mixture was then ignited with a spark flush with the test vessel end flange.

The flame travel was recorded by a centreline axial array of mineral insulated exposed junction type K thermocouples. The time of flame arrival was detected as a sharp change in the gradient of the voltage output of the thermocouple and in this way the average flame speed between any two thermocouples could be calculated. The pressure variation was recorded using a series of KELLER pressure transducers mounted at different places in both the explosion and dump vessels as shown in Figure 1. A fast (200 kHz per channel) 34 channel transient data acquisition system was used to record and analyse the data. A signal conditioning and processing package (FAMOS) was used to process the pressure signals. 10% methane with air (v/v) was used throughout this work. Each test was repeated at least 3 times and average readings were used.

RESULTS AND DISCUSSION

Pressure Records

Before the assessment of the influence of obstacles during vented explosions, a study of the unobstructed vented explosion was carried out. Figure 2 shows a pressure - time history and flame speed - time record with no obstacles. A number of pressure peaks are shown; two of them (P_1 and P_2) before the flame exited the tube (t_{out} on Figure 2 is the time at which the flame exited the tube). After the exit a number of oscillatory peaks were observed, the first of which usually reached the highest value and is marked as P_3 in Figure 2.

The initial overpressure P_1 was due to the initially inverted "U" shaped elongated flame observed in large L/D vessels where the flame accelerates towards the vent and is associated with high flame speeds due to the large flame surface area. Once the flame reached the tube wall the rate of production of burned gas volume rapidly decreased due to a large reduction in flame area, this produced a sudden reduction in the flame speed and thus the internal pressure fell. At this stage only unburned gas was being vented. The turbulence of the gas flow induced by the fast initial flame gave rise to a turbulent flame acceleration and the second pressure peak marked as P_2 in Figure 2. The pressure fell when the flame reached the vent. This was due to the onset of burned gas venting which led to a higher volumetric flow through the vent as well as due to the decreased flame area inside the vessel. When the flame reached the vent, the turbulent jet mixture of unburned gas previously vented was ignited and a third pressure peak, P_3, was observed. The magnitude of this pressure peak was the maximum overpressure in the system, $P_3 = P_{max}$. The pressure trace subsequent to the initial phase was strongly influenced by periodic acoustic oscillations set-up within the explosion tube.

Also shown in Figure 2 is the corresponding flame speed variation with time for the above test. Three major flame speeds were also observed connected with the above events; the first was at the same time with the first pressure peak the other two however were pressure waves travelling up and down in the tube moving the flame back and forth.

Although the third pressure peak, P_3, was the highest for $K_V = 1$ with an open end, it was the initial fast flame event resulting in pressure P_1 that was responsible for the events leading to P_2 and P_3. Additional work (in progress) has shown that if a vent with a bursting pressure is fitted then P_1 is increased by the burst pressure and then is the maximum overpressure at all L/D. Also if the vent area is less than the tube area, $K_V > 1$, then P_1 is always the maximum overpressure. The fast flame phenomena leading to P_1 are the same in fully closed vessel explosion of the same L/D, although the subsequent events resulting in pressures P_2 and P_3 are absent. Consequently, provided P_1 is the most important event in the vented explosion then predictions of the vented explosions with obstacles should be similar to closed vessel large L/D explosions with obstacles at the same position relative to the spark. Consequently, comparison of the present vented explosion results with the previous publication by Phylaktou and Andrews (3) will be made.

Figure 3 shows an explosion with the same mixture but with an orifice plate of 40% blockage at 6.8 tube diameters from the spark. Again three pressure peaks were identified and were attributed to the same events as with no obstacles, described above. However, P_2 was now much higher due to the additional turbulence caused by the obstacle. The first peak of the flame speed

also coincided with the first pressure peak (P_1), however, the subsequent flame peaks were out of time in relation to the pressure peaks (P_2 and P_3) and this was due to pressure waves interactions. Figure 4 shows a comparison of the pressure-time record for the different blockage ratios used in the present work. t_{ob} shown in this figure is the time (s) that the flame reached the obstacle. Clearly, an increase of the blockage ratio (BR) not only decreased the time of the explosion (i.e. faster explosion) but there was a significant increase in the maximum overpressure and in the rate of pressure rise.

The effect of the blockage on the three pressure peaks, mentioned above, is shown in Figure 5. For blockages below 60% a relatively small increase in the first pressure peak P_1 was recorded. This indicated that the initial elongated flame was essentially the same for this tests. However, for the highest blockage (80%) a significant increase in the first pressure peak was observed which was due to the restriction of the unburned gas flow by the large blockage. The second pressure peak (P_2) was attributed to the turbulence of the unburned gas flow induced by the flame. In the presence of the obstacle the gas flow interacted with it to generate more turbulence downstream of the obstacle. When the flame encountered this turbulence the combustion rate was increased resulting in faster production of burned gases and therefore a faster expansion rate and faster flame speed. This event is clearly shown in Figure 5 whereby an increase in blockage ratio significantly increased P_2 up to a blockage ratio of 60%. For the 80% blockage ratio, however this pressure peak was reduced, due to the restriction of the unburned gas flow by the large blockage and this reduced the turbulence downstream of the obstacle. This was also the reason for the sharp increase of the first pressure peak.

The reduced flame speed and pressure P_2 with the 80% blockage could have also been contributed to turbulent flame quenching resulting from excessive turbulence. It is generally accepted that there is a limiting value of the rms turbulent burning velocity above which the flame is quenched. Abdel-Gayed and Bradley (4) have correlated the experimental turbulent flame quenched data with the product K Le, where K is the Karlovitz stretch factor and Le is the Lewis number. For high turbulent Reynolds numbers ,R_ℓ, complete flame quenching occurred when K Le was larger than 1.5. Although, in the present work completely extinction was never recorded, the K Le product was 3.54 for a blockage ratio of 80%, well above the suggested limit of 1.5 for complete extinction to occur. All these turbulent parameters are discussed later in this paper.

The effect of the blockage ratio on the external explosion (P_3) is also shown in Figure 5. An increase of this overpressure was also obtained, with an increase in the blockage for up to 40%. However, for higher blockages this overpressure was decreased. This again, was due to the highly turbulent flame downstream of the obstacle burning the mixture in the tube faster than the unburnt mixture could be expelled. The pressure in the tube increased to 0.7 bar at 60% blockage so that a much greater mass of gas was burnt inside the tube and less energy was therefore utilised in the external explosion. The tube exit jet conditions were also due to sonic flow and the resulting jet flame also exhibited local quenching which could also have reduced P_3. For a closed tube the reduction in the P_2 overpressure at 80% blockage did not occur, indicating that local quenching did not occur. This could have been due to the higher pressure during this phase of the explosion and higher compression temperature. Increasing the pressure increases the turbulent Reynolds number, R_ℓ as the kinematic viscosity is inversely proportional to pressure. The compression temperature also increases the laminar burning velocity, S_L. Consequently, a different turbulent regime applies which may allow the flame to increase the propagation rate for a closed vessel but not for a vented vessel.

Flame speeds

The flame speeds for 10% methane in air explosions for different blockage ratios are shown in Figure 6 as a function of distance - to - diameter ratio (x/D). With the obstacle at 6.8D from the spark the fast initial flame speed, which occurred immediately upstream, induced high velocities in the unburned gas ahead of the flame and through the obstacle. This created turbulence downstream of the baffle. When the flame encountered this turbulence it became turbulent itself and accelerated to a maximum speed of 350 m/s for a blockage ratio of 60%. As the turbulence decayed, the flame decelerated, to almost its no-blockage value. The effect of the obstacle increased with increasing the blockage ratio for up to 60%. However, for higher blockage ratios, e.g. 80%, the peak flame speed was reduced for the reasons discussed above.

Figure 7 shows the maximum initial flame speeds upstream of the obstacle at different blockage ratios, as measured between the last two thermocouples before the obstacle. The flame speeds from the present work are compared with those obtained for completely closed vessels. It was previously established by Phylaktou and Andrews (3) that the higher the flame speed upstream of the obstacle the higher the turbulence was generated downstream the obstacle. During the present work, although a sharp decrease in the initial flame speed for a 20% blockage ratio, from that of no obstacle, was observed, for higher blockages the flame speed was almost constant whereas in a closed vessel there was a small reduction in the flame speed due to the restriction of the gas flow at large blockage. However, Figure 7 shows that the maximum initial flame speeds in a completely closed vessel and in a open-end vessel were of similar magnitude at 35-50 m/s.

The maximum flame speed downstream of the obstacle in the present tests were of the same order as those observed previously in a completely closed vessel by Phylaktou and Andrews (3). For example a maximum flame speed of 346 m/s was measured downstream of a single obstacle with a 70% blockage ratio compared to 354 m/s for a 60% blockage in the present work, for the same configuration and gas mixture.

Rates of pressure rise and enhancement factors

As was discussed earlier, the obstacles increased the turbulence which caused the increase in the second pressure peak (P_2). The rates of pressure rise due to the obstacle turbulence were normalised by dividing by the corresponding "no obstacle" rates. This produced an enhancement factor due to the obstacle, similar to the turbulence factor (β) used in vent design, Harris (5). These enhancement factors, determined by the normalisation of $(dP/dt)_2$, are shown in Figure 8 as a function of the blockage ratio. Also shown in this figure are the enhancement factors obtained in a totally closed vessel of the same L/D with the same obstacle. It can be seen that the enhancement factor was increased with an increase in the blockage ratio up to 60%. The decrease of the enhancement factor for higher blockage ratios was discussed earlier. The reduction of the enhancement factor at larger blockage ratio was absent in a totally enclosed vessel where a significant increase of the enhancement factor was measured for very large blockages as shown in Figure 8. The reason of this discrepancy is unknown but it could be due to different gas dynamics imposed by the absence of the end wall during the present work. However, similar enhancement factors due to the obstacles are shown in Figure 8, between the totally confined explosions and

totally open-end tube explosions, and this demonstrates the validity of assessing the effect of obstacles in totally enclosed tests.

Figure 9 shows the normalised overpressure P_2 obtained in the same way as the normalised rates of pressure rise. A similar trend as the normalised rates of pressure rise was obtained with a near linear increase up to a blockage ratio of 60%. Figure 9 shows the significance of turbulence created by a blockage on increasing the overpressure for end vented large L/D explosions with $K_V = 1$.

The present enhancement factors are up to twice the maximum factors recommended in the literature for severe cases of turbulence, Rasbash et al (1) and therefore a need for reviewing these guidelines is necessary. For large L/D vessels, Figure 8 gives an experimental basis for the evaluation of β for blockages up to 60%.

Turbulence Generation

Phylaktou and Andrews (6) presented a method for predicting the maximum turbulence levels generated downstream of a grid plate obstacle by an explosion induced flow. From theoretical considerations it was shown that the turbulence intensity, defined as the ratio of the rms turbulence velocity u′ to the mean velocity of the flow S_g, is simply given by the equation

$$u'/S_g = C_T\sqrt{K} \qquad (2)$$

where, K is the pressure loss coefficient and C_T is a constant equal 0.225 for "thin" or sharp-edged obstacles and 0.076 for "thick" or round-edged ones. The model was shown to predict available turbulence measurements in both transient (explosion generated) and steady state flows. The pressure loss coefficient K is defined as

$$K = \frac{\Delta P}{\frac{1}{2}\rho S_g^2} \qquad (3)$$

where ΔP is the total pressure loss due to the obstacle and ρ is the density of the fluid. For incompressible flow K can also be expressed in terms of the geometry alone as a function of the blockage ratio (BR) and the contraction coefficient (C_c).

$$K = \left(\frac{1}{C_c(1-BR)} - 1\right)^2 \qquad (4)$$

For a sharp edged orifice of high blockage $C_c \approx 0.61$; C_c depends on the blockage ratio and on the aspect ratio (t/d, thickness of plate/diameter of orifice) of the orifice. An empirical correlation of C_c by Ward-Smith (7) was combined with Eq. (4) to produce expressions for K independent of C_c

and dependent only on the geometrical characteristics of the orifice; the porosity ratio, p (1-BR), and the aspect ratio, t/d. For thin obstacles K is given by

$$K = \left[\frac{1}{0.608p\left(1 - p^{2.6}\right)\left[1 + (t/d)^{3.5}\right] + p^{3.6}} - 1 \right]^2 \qquad (5)$$

for data in the ranges of

$0 < t/d < 0.6, \qquad 0 < p < 0.75, \qquad 0.57 < K < 35000$

Turbulent combustion

When a turbulent mixture is ignited combustion is faster than when the same mixture is burning in a laminar mode. How much faster a turbulent mixture burns is expressed in terms of the turbulence factor β which is defined as the ratio of turbulent to laminar burning velocities, i.e. Eq (1).

The correlation of β to turbulent flow characteristics and the combustion properties of the mixture has been the subject of intensive research in recent years but an exact correlation has been eluding researchers. For methane air mixtures, Phylaktou (8) produced the following turbulent combustion correlation on the basis of a large set of experimental data from explosions with obstacles

$$\frac{S_T}{S_L} - 1 = 0.67 \left(\frac{u'}{S_L} \right)^{0.47} R_\ell^{0.31} \qquad (6)$$

R_ℓ is the turbulent Reynolds number defined as

$$R_\ell = \frac{u'\ell}{\nu} \qquad (7)$$

where ℓ is the integral length scale of turbulence which is equal to the width of the rim of the orifice plates used in this project, Phylaktou (8). Using Eq. (7) in conjunction with Eq. (2) the combustion downstream of the obstacle could be characterised and thus the turbulent combustion factor could be evaluated.

For a constant length scale or similar variation in ℓ ,Phylaktou et al (9) have shown that most turbulent data fit the empirical expression

$$\frac{S_T}{S_L} - 1 = 2\frac{u'}{S_L} \qquad (8)$$

Combining equations 8, 2 and 4 shows that

$$\frac{S_T}{S_L} - 1 = 2C_T\sqrt{K}\frac{S_g}{S_L} = 2C_T\frac{S_g}{S_L}\left(\frac{1}{C_C(1-BR)} - 1\right) \qquad (9)$$

Equation 9 shows that S_T is directly related to the obstacle blockage and the upstream flow velocity as the two most important parameters.

Upstream gas-velocities

Three differential pressure transducers were employed to provide information about the induced flow, S_g, patterns within the test geometry, positioned as shown in Figure 1. DP1 was intended to provide a qualitative picture of the pressure difference between the ignition vessel and the dump vessel. DP2 was to measure the pressure drop across the obstacle which is the pressure difference on which the calculation of the gas flow through an orifice is usually based. Upstream and downstream pressure tappings according to BS1042 (10) for orifice plate flow metering were used. This pressure drop is recovered to an extend farther downstream and this residual pressure loss due to the presence of the obstacle was to be measured by DP3. This pressure loss represents the energy lost from the flow due to the generation of flow turbulence and the subsequent dissipation of turbulence energy into heat and random molecular motion. This pressure loss ΔP is the quantity that determines the pressure loss coefficient in Eq. (3) and whose relation to the maximum turbulence levels have been described above.

The British Standards BS1042 (10) specify that for flow metering the orifice blockage should not be lower than 50%, therefore, only for blockage ratios of 60% and 80% are the measurements reliable. An attempt to measure the pressure difference for lower blockage was unsuccessful due to not as good as expected performance of the differential pressure transducers. The reading of interest in the present experiments was the maximum pressure difference ΔP just before the flame arrival at the obstacle. Figure 10 shows a comparison of the induced gas velocities through the obstacle between a completely closed and open-end vessel. Although, during the present work the initial flame speeds were slightly higher, the induced gas velocities through the obstacle were slightly lower from those measured in a completely closed vessel.

Estimation of S_T/S_L from S_g

With all parameters known, first the rms turbulence intensities (u'/S_g) were calculated using Eq. (2) and then the turbulent Reynolds number (R_ℓ) using Eq. (7). The turbulence factors defined as the turbulent to laminar burning velocity (S_T/S_L) was then evaluated using Eq. (6). These turbulent-combustion parameters which characterise the explosions with obstacles in the present project are shown in Table 1.

Table 1. Turbulent combustion parameters.

BR (%)	$(dP/dt)_2$ Norm.	ΔP (mbar)	Flame Speed (m/s)	S_g (m/s)	R_ℓ	u'/S_L	S_T/S_L Eq. 6	S_{Tob}/S_{Tno}	S_T/S_L Eq. 11
60	25	46.92	50	23.72	13694	34	68	9	26
80	19	150.36	48	18.85	40315	67	131	17	40

The turbulent factors (β) calculated using Eq. (6) are higher compared to those obtained from the normalised rates of pressure rise. This was because the flame propagation in the absence of an obstacle was not laminar. At the high unburnt gas velocities, induced by the fast flame, the unburnt gas Reynolds number was highly turbulent. For the empty tube the maximum unburnt gas velocity calculated from the exit pressure loss (PB-PC) equated to the dynamic head pressure loss was 24.6 m/s giving a tube Reynolds number of Re = 118848. Abdel-Gayed and Bradley (11) have correlated the turbulent Reynolds number R_ℓ as a function of tube Reynolds number by Equation 10.

$$R_\ell = 13.45 \times 10^{-3}\ Re^{0.902} \tag{10}$$

This equation gives an R_ℓ = 509, and from Equation 6 an S_T/S_L = 7.83 The influence of the obstacle can now be predicted by using the ratio of the predicted S_T with obstacle to S_T for the empty tube (S_{Tob} / S_{Tno}). The ratio is given in Table 1 and shows a much better agreement with the experimental normalised rates of pressure rise.

A commonly used turbulent burning velocity correlation is that by Bradley et al (12) and given by

$$\frac{S_T}{S_L} = 1.53\, Le^{-0.3} \left(u'/S_L\right)^{0.4} R_\ell^{0.15} \tag{11}$$

where Le is the Lewis number which is equal to 1 for methane/air explosions. The predictions of this correlation are also shown in Table 1. It can be seen that Eq. 11 gives a good comparison with these factors determined from the normalised rates of pressure rise. However, this is a fortuitous agreement as the flame without the obstacle is not laminar.

Exit gas flow

The pressure loss across the vent opening (PB-PC) determines the mass flow rate through the opening. This pressure loss is characteristic of the vent area and the velocity of the flow. It is usually expressed in a non-diamensionless form as the pressure loss coefficient, K, defined by the following equation

$$K = \frac{\Delta P}{\frac{1}{2}\rho S_g} = 1 \tag{12}$$

During the present work the pressure loss across the vent could be obtained by subtracting the pressure transducer signal of PC from that of the pressure transducer signal PB. The pressure loss, ΔP, obtained in this way could be used in equation 12 to evaluate the induced gas velocities through the vent. These maximum induced gas velocities are given in Table 2 together with the calculated turbulent parameters. It is clear that an increase in the blockage ratio decreases the flow of the unburned gas through the vent and therefore the magnitude of the external explosion is reduced as was shown in Figure 5.

Table 2. Induced gas velocities through the vent and calculated turbulent parameters.

BR(%)	ΔP (mbar)	Flame Speed downstream (m/s)	S_g (m/s)	R_ℓ	u'/S_L	S_T / S_L
0	3.42	134	24.64	509	2.29	7.83
20	157.41	215	103.25	2081	7.97	19.98
40	81.16	321	94.91	1814	7.46	16.64
60	79.89	353	92.04	1763	7.26	18.26
80	40.38	318	63.53	1220	5.26	14.24

CONCLUSIONS

The effect of obstacles during open-ended explosion have been assessed. During an unobstructed explosion three major pressure peaks were identified: P_1 due to the elongated flame which is typical of explosions in large L/D vessels, P_2 due to the turbulence of the unburned gas and P_3 due to the external explosion. With the obstacle in place the same three pressure peaks were present but the magnitude of the second pressure peak (P_2) was increased significantly with an increase in blockage ratio up to 60%. This increase was due to an increase in turbulence of the unburned gas flow downstream of the obstacle. For higher blockage ratios (80%) this pressure peak was decreased due to the reduction of the unburned gas flow by the large blockage as well as due to local flame quenching at the very high turbulence levels. The normalised rates of pressure rise were found to be of the same order as those in completely closed vessel, previously reported. The turbulent factors were calculated from the estimates of the turbulent burning velocities and these compared well with the enhancement factors obtained from the normalised rates of pressure rise. These turbulent factors were found to be at least twice higher than those suggested in the literature for severe explosions.

Current recommendations for venting explosions in large L/D vessels with obstacles, such as those contained in the NFPA 1988 (2) are fairly arbitrary and based on very little experimental work. The work reported here goes some way in providing quantitative data for this set up. However, further work is needed to assess the influence of vent position relative to the obstacle and also of vent area and vent breaking pressure, before guidelines for the explosion relief of these systems may be given. Some of this work is currently under progress in this laboratory.

ACKNOWLEDGEMENT

We would like to thank the EPSRC for research grant H/40914 in support of this work.

REFERENCES

1. Rasbash, D. J., Drysdale, D. D. and Kemp, N., 1976 IChemE. Sympos. Series No. 47.
2. NFPA 68, 1988 Venting Of Deflagrations, National Fire Prevention Association.
3. Phylaktou, H. and Andrews, G.E., 1991 Combust Flame, 85 p.363.
4. Abdel-Gayed, R. G., and Bradley, D., 1985 Combust Flame, 62 p.61.
5. Harris, R.J. 1983 Gas Explosions In Buildings And Heating Plants, British Gas Corporation and E&FN Spon. London and New York.
6. Phylaktou, H. and Andrews, G. E., 1994 25th Intern. Sympos. on Combustion p 103.
7. Ward Smith, A. J., 1971 Pressure Loss In Ducted Flows, London Butterworths.
8. Phylaktou, H., 1993 PhD Thesis, University of Leeds.
9. Phylaktou, H., Andrews, G. E. Mounter, N. and Khamis, K. M., 1992 IChemE Sympos. Series No 130 p. 525.
10. BS1042, 1981 British Standards Institute.
11. Abdel-Gayed, R. G. and Bradley, D., 1981 Proc. R. Soc. Lond. A 301 p. 1.
12. Bradley, D., Lau, A. K. C. and Laws, M., 1992 Phil. Trans. R. Soc. London A338 p. 359.

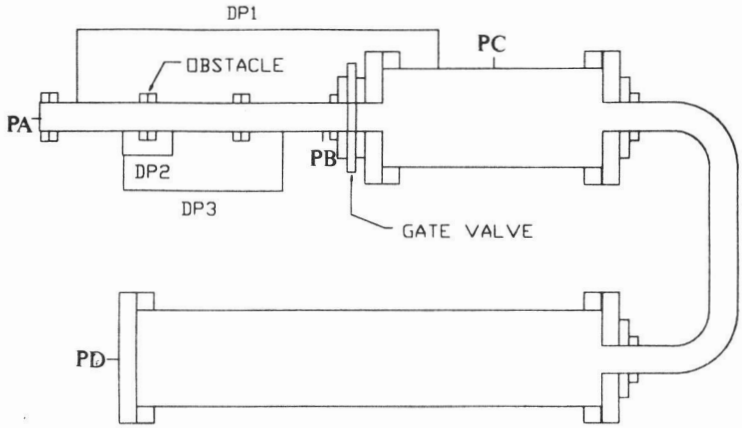

Figure 1. Schematic representation of the test rig and pressure instrumentation.

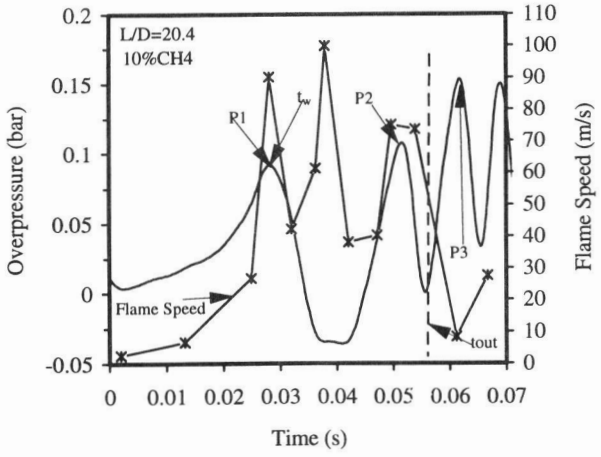

Figure 2. Pressure - time history and flame speed - time record for 10 % methane in air with no obstacle.

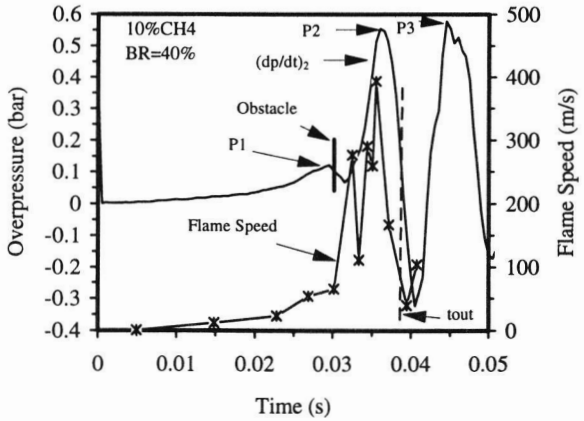

Figure 3. Pressure - time history and flame speed - time record for 10 % methane in air with blockage ratio of 40%.

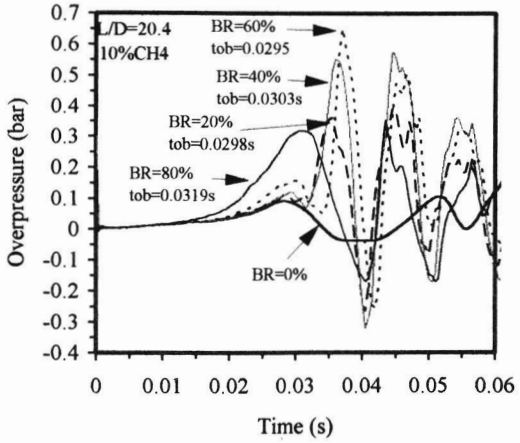

Figure 4 A comparison of the pressure - time records for the different blockage ratios used in the present work.

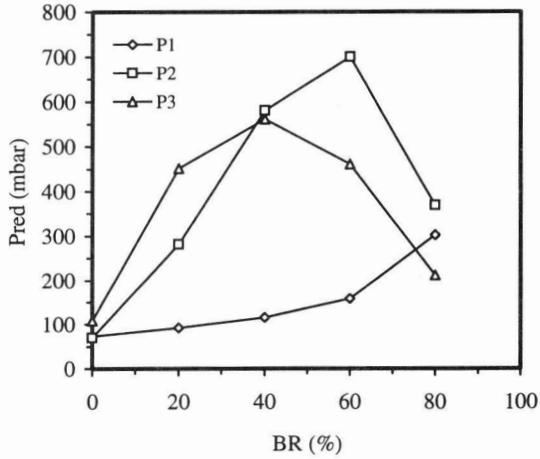

Figure 5. The effect of the blockage ratio on the three pressure peaks identified in the present work.

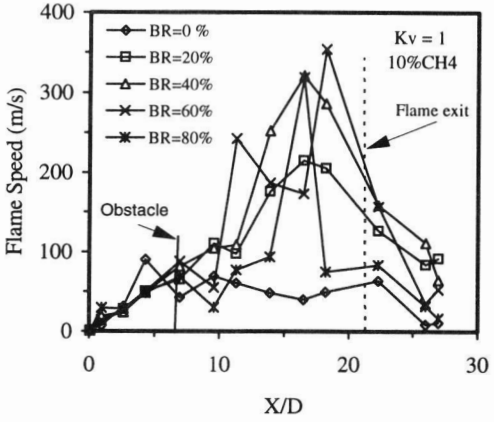

Figure 6. Flame speeds as a function of distance to diameter ratio (X/D) for different blockage ratios.

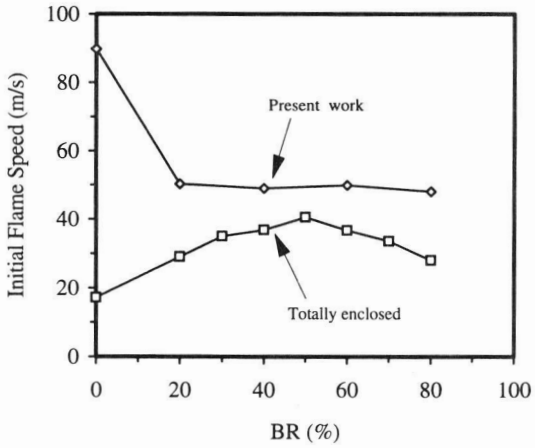

Figure 7. A comparison of the initial flame speed as a function of the blockage ratio between the present work and the totally closed vessel work.

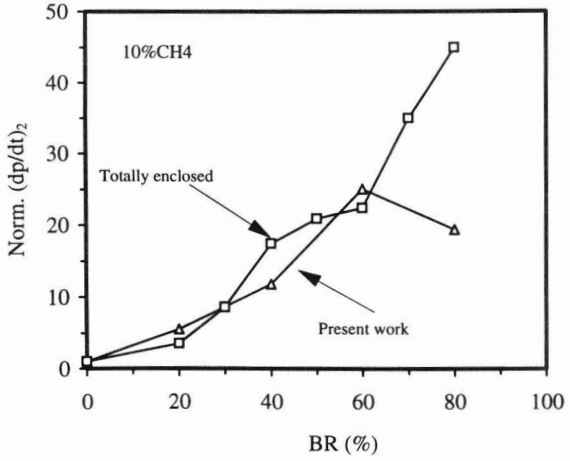

Figure 8. A comparison of the normalised rates of pressure rise due to the obstacle $(dP/dt)_2$ between the present work and the totally closed vessel work.

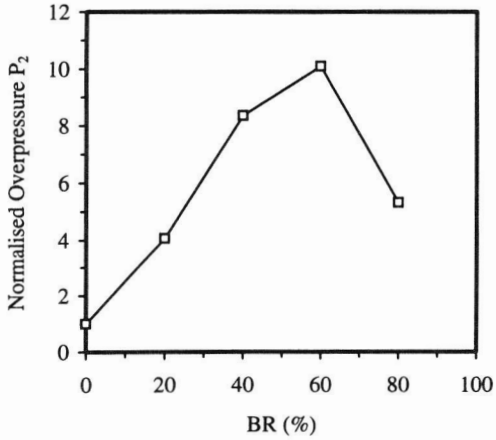

Figure 9. Normalised overpressure P_2 as a function of the blockage ratio.

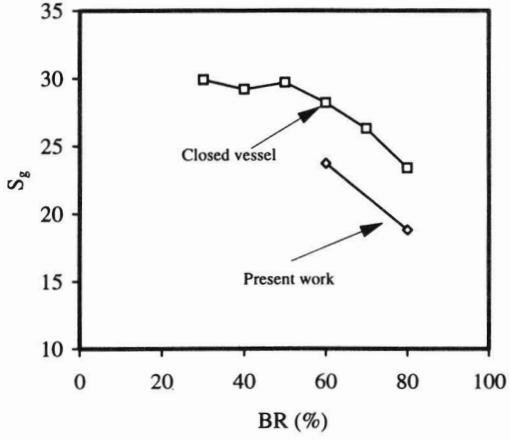

Figure 10. A comparison of the induced gas velocities as a function of the blockage ratio between the present work and the totally closed vessel work.